Applied Surface Science 282 (2013) 297–301

Contents lists available at SciVerse ScienceDirect

Applied Surface Science

journal homepage: www.elsevier.com/locate/apsusc

Determination of non-uniform graphene thickness on SiC (0 0 0 1) by X-ray diffraction

A. Ruammaitree*, H. Nakahara, K. Akimoto, K. Soda, Y. Saito

Department of Quantum Engineering, Faculty of Engineering, Nagoya University, Nagoya 464-8603, Japan

ARTICLE INFO

Article history:
Received 21 March 2013
Received in revised form 17 May 2013
Accepted 24 May 2013
Available online 2 June 2013

Keywords:
SiC
Epitaxial graphene
X-ray diffraction
Angle-resolved photoemission spectroscopy

ABSTRACT

Epitaxial graphene thickness distribution grown on Si-terminated SiC (0 0 0 1) surface was analyzed by using an X-ray diffraction (XRD) pattern and a simple equation. These results were confirmed by low accelerating voltage scanning electron microscopy and angle resolved photoemission spectroscopy. Despite its simplicity, proposed XRD analysis provides fairly accurate information on layer spacing and thickness distribution of graphene layers. It is expected that this method is useful for quick evaluation of graphene layer numbers on large scale substrate.

1. Introduction

Graphene is an allotrope of carbon created by arrangement of carbon atoms in a two-dimensional honeycomb lattice. The unit cell of graphene, in which two carbon atoms are contained, is formed by two lattice vectors, $|a_G| = |b_G| = 2.4589$ Å [1,2]. In the electronic band structure, graphene has two important bonding types which are π bond (perpendicular to the planar sheet) and σ bond (in-plane sheet). Graphene also has many exotic properties such as high mobility and linear dispersion (Dirac cone) at the *K*-point in the Brillouin zone where the valence and conduction band touch each other [3–5]. These unique properties of graphene make it a promising candidate for the future electronic [6,7] and photonic devices [8].

Graphene can be formed by many ways such as mechanical exfoliation of graphite, chemical vapor deposition (CVD) of carbon-bearing gases on the surface of copper films [9], and cutting open nanotubes [10]. The growth of graphene by annealing SiC substrate is also one of the efficient approaches for a large scale production of graphene. The estimation of the graphene film thickness on SiC substrate is necessary since the properties of graphene depend on its thickness. In general, there are several techniques, such as scanning electron microscope (SEM) [11], Auger electron spectroscopy (AES) [12,13], X-ray photoelectron spectroscopy (XPS) [14], attenuation of substrate Raman intensity [14], angle-resolved photoemission spectroscopy (ARPES) [1] and surface X-ray diffraction (SXRD) [15,17] to determine the layer number of graphene grown on SiC. For the AES and XPS, the thickness determination relies on the Si/C intensity ratio and the model which assumes that graphene is grown uniformly on SiC substrate. Their accuracy could suffer from the unrealistic model and the inaccurate knowledge of the inelastic mean free path of electrons [12–14,18]. In the case of the estimation by attenuation of substrate Raman intensity, the accuracy depends on the Raman intensity of SiC which varies in position. In the case of ARPES, it can reveal the graphene band structure which implies only the combination of graphene layer but not respective coverages. The SXRD is a wonderful method which can estimate the film thickness. Nevertheless, this method is rather complicated and time consuming, that is the SXRD needs hundreds of truncation rod intensity measurements (which takes tens of hours) [16,17] and also needs many fitting parameters (such as 3-dimensional atomic positions of each atoms including interface and SiC layers and surface roughness) for structural analysis [15]. In particular, large number of parameters causes many candidates of best fit parameter sets as well as time consuming analysis. Low accelerating voltage SEM (LV-SEM) is a technique which can locally distinguish the relative graphene thickness regions by difference in contrast but it cannot exhibit the absolute graphene thickness unless contrast-thickness relation for each sample is obtained.

In this report, an X-ray diffraction (XRD) pattern around a graphene peak was used for layer number distribution determination of non-uniform graphene layers on SiC substrate. The XRD pattern was analyzed by using a simple equation and few numbers

* Corresponding author. Tel.: +81 8038233199.
E-mail addresses: akkawat@surf.nuqe.nagoya-u.ac.jp, u4605070@hotmail.com (A. Ruammaitree).

0169-4332/$ – see front matter © 2013 Elsevier B.V. All rights reserved.
http://dx.doi.org/10.1016/j.apsusc.2013.05.122

of parameters (such as layer spacing and layer coverage of graphene film). The XRD results were compared with LV-SEM and ARPES for confirmation.

2. Experimental

N-type Si-terminated 6H-SiC (0 0 0 1) substrates were employed for the graphene growth. The substrate was precleaned by ultrasonic in acetone. After acetone was evaporated, the substrate was immediately mounted on the sample holder and put in the main chamber with the base pressure of $\sim 10^{-8}$ Pa followed by silicon deposition (about 2 layers) on the substrate. After that the substrate was transferred to an argon chamber without exposure to air and then annealed in argon gas with a pressure of 0.05, 0.3 and 0.5 atm. The samples were named as the value of argon pressure where they were annealed in. The annealing temperature was in range from ~900 °C to graphitization temperature (1550 °C for the 0.05 atm sample, 1675 °C for the 0.3 atm sample and 1700 °C for the 0.5 atm.sample) with increasing temperature by ~100 °C. The annealing time was about 10–15 min for each temperature to produce a few layered graphene. The sample heating was carried out by direct current through the sample.

After annealing, an ex situ XRD measurement was carried out at the beam line 4C, Photon Factory, KEK (Tsukuba, Japan). Diffraction data were collected at X-ray energy of 10.2 keV and incident beam size of 1 mm at room temperature. An ARPES measurement was also conducted at room temperature at the beam line 5U of UVSOR-II in the Institute for Molecular Science, Okazaki, Japan. The excitation photon energy was set to 80 eV. An ultra-high vacuum (UHV)-SEM (Omicron Nano Technology) observation with incident beam of 1.7–2.2 keV was also carried out.

3. Results and discussion

Fig. 1 shows XRD profiles (blue dots) of graphene films grown on SiC under argon pressure of (a) 0.05 atm, (b) 0.3 atm, and (c) 0.5 atm. As indicated in the figure, diffraction peaks of graphene layers and SiC are observed at ~20° and 27.8°, respectively. The *d*-spacings of the SiC can be calculated from the peak position as about 2.51 Å, which corresponds to SiC bilayer spacing (2.52 Å) [1].

To estimate graphene thickness from XRD profiles, Laue diffraction function were used. At first, a simple model was assumed that the graphene was grown uniformly on SiC substrate. Under this assumption, the following simple equation was used for profile calculation.

$$|F|^2 \propto |f(\theta)|^2 \left| \sum_{j=0}^{N} e^{ika_j j} \right|^2 . \quad (1)$$

Here, F is a structure factor, N is the number of graphene layer, and $f(\theta)$ is an atomic scattering factor which can be taken from Ref. [19]. $ka_j = (4\pi d_j \sin\theta)/\lambda$ where d_j is a lattice spacing (between jth and $(j-1)$th layers) perpendicular to the surface, θ is an angle between the incident ray and the scattering planes, λ is a wavelength of X-ray. In order to avoid the effect of SiC substrate, the fitting was operated in the range of 2θ from 10 to ~22°. Green dotted line and red broken line in Fig. 1(a) are calculated curves from Eq. (1) with graphene layer number (N) of 1 and 2, respectively. The spacing d of 3.60 Å was employed. As shown in the figure, there are large discrepancy between the calculated curve and the experimental one, i.e. too broad for $N = 1$ or too narrow for $N = 2$. This suggests that the number of graphene layers on the SiC substrate is not uniform, but has a distribution.

In order to improve the fitting, another model which includes graphene thickness distribution was introduced as shown in Fig. 2. With this model and the Laue functions, XRD intensity can be calculated as

$$|F|^2 \propto |f(\theta)|^2 \left| \sum_{j=0}^{N} \beta_j e^{ika_j j} \right|^2 , \quad (2)$$

where β_j is a occupancy of jth graphene layer (its value is between 0 and 1). Solid lines in Fig. 1(a)–(c) show results of fitting by using Eq. (2). Parameters (d_j and β_j) used in those calculations are shown in Table 1. It is apparent that the curve obtained from the modified model exhibits better fitting than those of the uniform model. χ^2 ($=\sum(O-E)^2/E$; O is intensity from the calculation, E is that from experiment) dependence on β_j parameter change is shown in Fig. 1(d). It reveals steep valley which suggests the fitting resolution is good enough (less than 2%). For the interlayer spacings d_j,

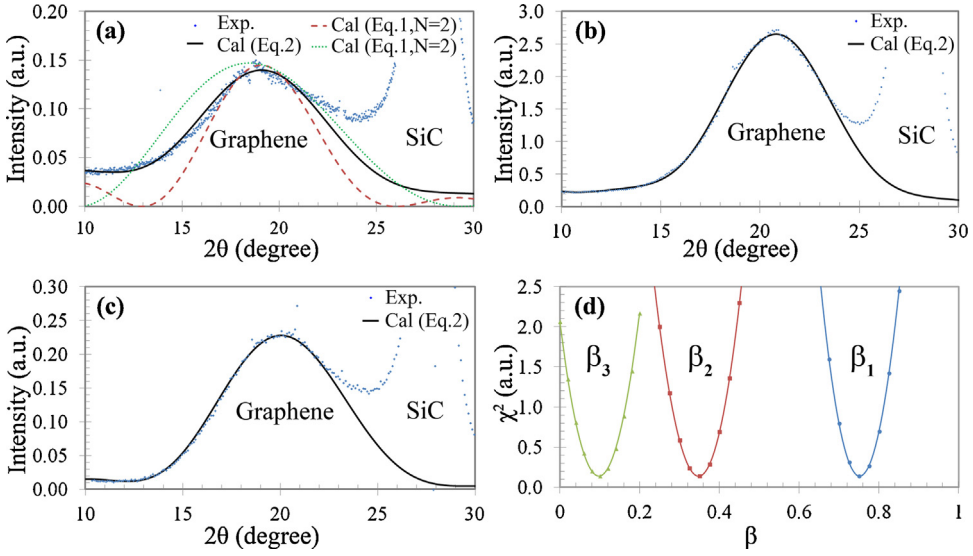

Fig. 1. Experimental XRD profiles (blue dots) of graphene films grown on SiC (0 0 0 1) surface, which was annealed under argon pressure of (a) 0.05, (b) 0.3 and (c) 0.5 atm. As written in the figures, peaks at ~20° and 27.8° correspond to graphene layers and SiC bilayers respectively. Green dotted line and red broken line in (a) are calculated results using fitting Eq. (1) with parameters $N = 1$ and $N = 2$, respectively. A solid line in each figure shows a calculated result using Eq. (2) and (d) the chi-squared (χ^2) dependence on β_j parameters for 0.3 atm sample. (For interpretation of the references to color in this figure legend, the reader is referred to the web version of the article.)

Table 1
XRD fitting parameters, d_j's (inter layer spacing) and β_j's (occupancy of jth graphene layer).

Ar pressure	0.05 atm		0.3 atm			0.5 atm	
j	1	2	1	2	3	1	2
d (Å)	3.55 ± 0.05	3.50 ± 0.05	3.30 ± 0.05	3.30 ± 0.05	3.30 ± 0.05	3.40 ± 0.10	3.40 ± 0.05
β (%)	47 ± 2	14 ± 2	75 ± 5	35 ± 5	10 ± 5	90 ± 5	36 ± 5

there is one thing to point out. d value for bulk graphite is known as 3.35 Å and fittings result for 0.3 and 0.5 atm.samples agree with this value. While for 0.05 atm sample, calculated d values are about 3.5 Å and about 5% larger than that of the bulk value. The reason of the increase in interlayer spacing of this sample is not clear but similar values were also obtained by X. Weng group measured by a high-resolution high-angle annular-dark-field (HAADF) scanning TEM (STEM) [20]. Coverages of n-layers graphene regions (θ_n) can be calculated from β values as $\theta_n = \beta_n - \beta_{n+1}$, and those results are shown in the "by XRD" line in Table 2.

To confirm layer number distribution obtained by XRD analysis, low acceleration UHV-SEM experiments were carried out. Fig. 3 shows respective SEM images for 0.05, 0.3 and 0.5 atm.samples. As shown in the figure, there are clear contrasts on the sample surfaces (indicated by 0, 1, and 2 in the figure). As described in the introduction, SEM contrast corresponds to number of layer of graphene. However, absolute values of numbers cannot be determined. To overcome this weakness, the following procedure was carried out. Samples used in this experiment were heated by direct current, so that sample area near electrode could not be heated as high as graphitization temperature. Thus SiC surface remains in this area. Therefore continuous observation from SiC area to graphitized area gives contrast-layer number relation for each sample. As a result, it was confirmed that area 0, 1 and 2 in SEM images correspond to buffer layer, monolayer and bilayer graphene regions. Unfortunately, it was impossible to distinguish more than 2 layers region from bilayer region under our experimental condition (acceleration voltage, S/N etc.). It is also a problem to compare XRD and SEM results that observation area is different, ~1 mm for XRD and ~10 μm for SEM. Therefore SEM measurements were carried out at several points within XRD measurement area, and area of each contrast was summed up. Coverage of n-layers graphene region obtained by SEM images are show in "by SEM" line in Table 2. As shown in the table, coverages determined by XRD analysis are in good agreement with those measured by SEM.

For qualitative inspection, ARPES experiment was also carried out and its result is shown in Fig. 4. The sample used in this experiment is graphene grown under 0.05 atm of Ar pressure, which was determined as mixture of 33% monolayer and 14% bilayer graphene using the XRD analysis. Here, the origin of the energy axis is taken at the Fermi energy E_F. The inset curves at the bottom

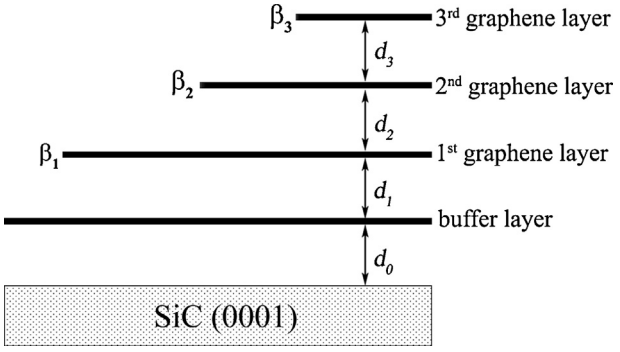

Fig. 2. Schematic of thickness distribution model used in Eq. (2). β_0 is assumed as 1.

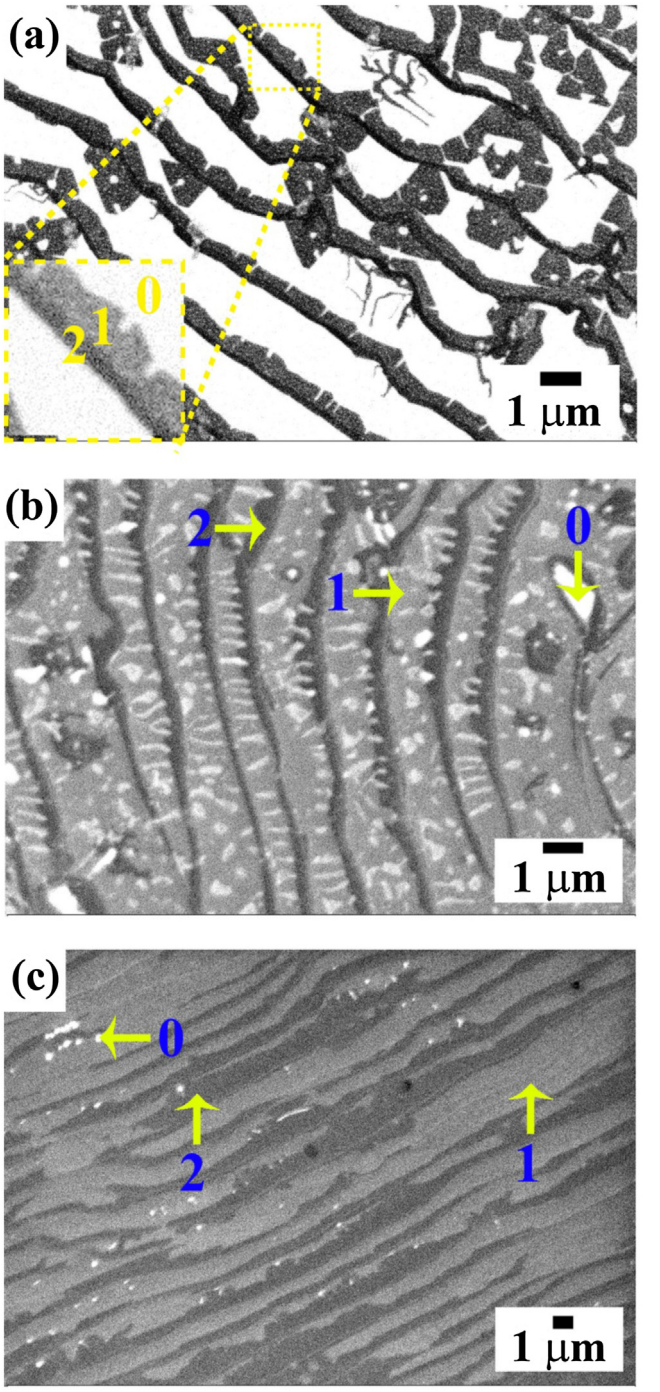

Fig. 3. Low accelerating voltage UHV-SEM images of (a) 0.05, (b) 0.3 and (c) 0.5 atm.samples taken with accelerating voltage of 2.2, 2.2 and 1.7 kV, respectively. There are 3 contrast levels in these images, bright (indicated 0 in the figure), dark gray (1), and black (2), those correspond to buffer layer, monolayer and bilayer graphene, respectively. Inset figure in (a) is the magnified image in the broken line square. The image contrast was adjusted to make a distinction of graphene thickness clearly.

Table 2
Coverages of *n*-layers graphene regions determined by XRD and SEM.

Ar pressure	0.05 atm				0.3 atm				0.5 atm			
Layers (*n*)	Buffer (0) (%)	Monolayer (1) (%)	Bilayer (2) (%)		Buffer (0) (%)	Monolayer (1) (%)	Bilayer (2) (%)	Trilayer (3) (%)	Buffer (0) (%)	Monolayer (1) (%)	Bilayer (2) (%)	
By XRD	53	33	14		25	40	25	10	10	54	36	
By SEM	53	41	6		25	48	27		4	58	38	

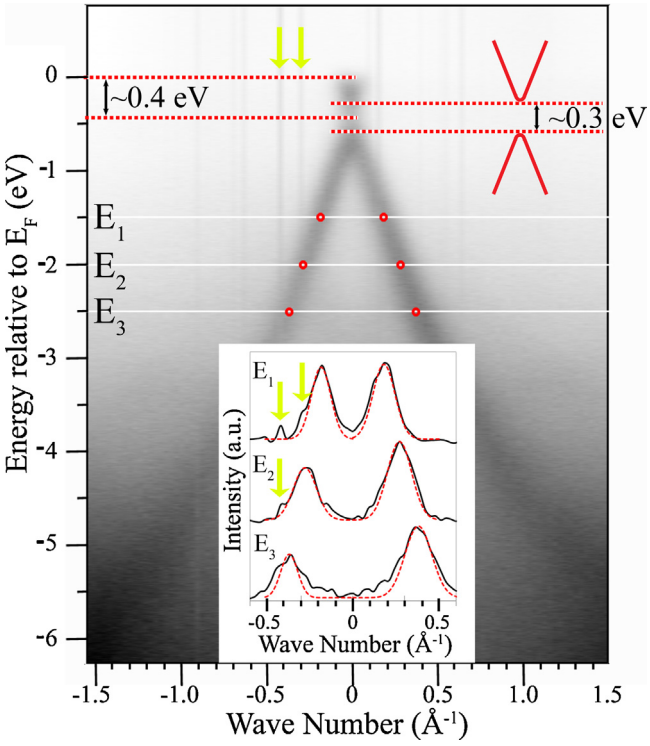

Fig. 4. ARPES spectra of the 0.05 atm sample around the *K* point of graphene. Upper right illustration represents a schematic electronic band structure which originated from a graphene monolayer. An inset at the bottom shows momentum distribution curves of photoelectrons at the energies of −1.5, −2 and −2.5 eV. Broken lines in the graph show the components of the monolayer electronic structures fitted using Gaussian functions. Vertical arrows indicate two of noise signal lines (both in ARPES mapping and the inset graph).

of Fig. 4 display intensities of photoelectrons with energies of −1.5, −2 and −2.5 eV against wave number (the momentum distribution curve). The intensity profile was fitted by Gaussian functions, and the results were shown by broken lines. In this fitting noise peaks indicated by vertical arrows were ignored. The electronic band obtained by ARPES experiment consists of a single branch as shown by the fitting result, which implies this sample consists of monolayer graphene [1]. However, the band apparently shows a band gap (~0.3 eV) and binding energy shift (~0.4 eV), which is different from free standing graphene monolayer [5]. It is considered that the band gap opening and the energy shift are caused by interaction (strain and/or doping) between monolayer graphene and the substrate [21]. Since ARPES evaluates only graphene layers (but not a buffer layer). It can be said that majority of graphene area is monolayer region. However, it is very difficult to obtain quantitative value of layer distribution. XRD analysis delivered that 70% (33/(33 + 14)) of graphene region of this sample is monolayer, which is qualitatively consistent with the ARPES result.

4. Conclusion

In this report we offer the new method to deliver absolute and reliable information on graphene thickness distribution on SiC substrate using XRD experiments and simple Laue functions. Unlike other methods like low acceleration SEM, this is a standardless method i.e. you do not need a standard or a known sample to determine absolute values of layer number distributions. However, it still has a limitation since the graphene peak is only considered. This approach is, therefore, suitable for the sample on which at least 1 carbon layer (buffer layer) covers the whole area shone by an X-ray beam.

Acknowledgements

The XRD measurements were supported by Photon Faculty, High Energy Accelerator Research Organization, Tsukuba, Ibaraki Prefecture, Japan. The ARPES measurements were performed at the Institute of Molecular Science, Okazaki, Aichi Prefecture, Japan.

References

[1] J. Hass, W.A. de Heer, E.H. Conrad, The growth and morphology of epitaxial multilayer graphene, Journal of Physics: Condensed Matter 20 (2008) 323202.
[2] Y. Baskin, L. Meyer, Lattice constants of graphite at low temperatures, Physical Review 100 (1955) 544.
[3] K.V. Emtsev, F. Speck, Th. Seyller, L. Ley, Interaction, growth, and ordering of epitaxial graphene on SiC{0 0 0 1} surfaces: a comparative photoelectron spectroscopy study, Physical Review B 77 (2008) 155303.
[4] T. Ohta, A. Bostwick, J.L. McChesney, Th. Seyller, K. Horn, E. Rotenberg, Interlayer interaction and electronic screening in multilayer graphene investigated with angle-resolved photoemission spectroscopy, Physical Review Letters 98 (2007) 206802.
[5] A.K. Geim, A.H. MacDonald, 5 graphene: exploring carbon flatland, Physics Today 60 (2007) 35.
[6] S. Wang, J. Wang, P. Miraldo, M. Zhu, R. Outlaw, K. Hou, X. Zhao, B.C. Holloway, D. Manos, High field emission reproducibility and stability of carbon nanosheets and nanosheet-based backgated triode emission devices, Applied Physics Letters 89 (2006) 183103.
[7] H.B. Heersche, P.J. Herrero, J.B. Oostinga, L.M.K. Vandersypen, A.F. Morpurgo, Bipolar supercurrent in graphene, Nature 446 (2007) 56.
[8] F. Bonaccorso, Z. Sun, T. Hasan, A.C. Ferrari, Graphene photonics and optoelectronics, Nature Photonics 4 (2010) 611.
[9] A. Ismach, C. Druzgalski, S. Penwell, A. Schwartzberg, M. Zheng, A. Javey, J. Bokor, Y. Zhang, Direct chemical vapor deposition of graphene on dielectric surfaces, Nano Letters 10 (2010) 1542.
[10] L. Jiao, L. Zhang, X. Wang, G. Diankov, H. Dai, Narrow graphene nanoribbons from carbon nanotubes, Nature 458 (2009) 877.
[11] H. Hiura, H. Miyazaki, K. Tsukagoshi, Determination of the number of graphene layers: discrete distribution of the secondary electron intensity stemming from individual graphene layers, Applied Physics Express 3 (2010) 095101.
[12] S.N. Luxmi, P.J. Fisher, R.M. Feenstra, G. Gu, Y. Sun, Temperature dependence of epitaxial graphene formation on SiC(0 0 0 1), Journal of Electronic Materials 38 (2009) 718.
[13] W.A. de Heer, C. Berger, X. Wu, P.N. First, E.H. Conrad, X. Li, T. Li, M. Sprinkle, J. Hass, M.L. Sadowski, M. Potemski, G. Martinez, Epitaxial graphene, Solid State Communications 143 (2007) 92.
[14] S. Shivaraman, M.V.S. Chandrashekhar, J.J. Boeckl, M.G. Spencer, Thickness estimation of epitaxial graphene on SiC using attenuation of substrate Raman intensity, Journal of Electronic Materials 38 (2009) 725.
[15] J. Hass, R. Feng, J.E. Millan-Otoya, X. Li, M. Sprinkle, P.N. First, W.A. de Heer, E.H. Conrad, Structural properties of the multilayer graphene/4H-SiC ($0\,0\,0\,\bar{1}$) system as determined by surface X-ray diffraction, Physical Review B 75 (2007) 214109.
[16] Q. Shen, J.M. Blakely, M.J. Bedzyk, K.D. Finkelstein, Surface roughness and correlation length determined from X-ray-diffraction line-shape analysis on germanium (1 1 1), Physical Review B 40 (1989) 3480.
[17] I.K. Robinson, Crystal truncation rods and surface roughness, Physical Review B 33 (1986) 3830.
[18] H. Hibino, H. Kageshima, M. Nagase, Epitaxial few-layer graphene: towards single crystal growth, Journal of Physics D: Applied Physics 43 (2010) 374005.
[19] P. Brown, A. Fox, E. Maslen, M. O'Keefe, B. Willis, International Tables for Crystallography C (6) (2004) 554, http://dx.doi.org/10.1107/97809553602060000600.
[20] X. Weng, J.A. Robinson, K. Trumbull, R. Cavalero, M.A. Fanton, D. Snyder, Structure of few-layer epitaxial graphene on 6H-SiC (0 0 0 1) at atomic resolution, Applied Physics Letters 97 (2010) 201905.
[21] Z.H. Ni, T. Yu, Y.H. Lu, Y.Y. Wang, Y.P. Feng, Z.X. Shen, Uniaxial strain on graphene: Raman spectroscopy study and band-gap opening, ACS Nano 2 (2008) 2301.